Deconvoluting structures of component plant biopolymers using deuterium labeled Brassica oleracea stems

Journal:	*ACS Sustainable Chemistry & Engineering*
Manuscript ID	sc-2023-04076h.R3
Manuscript Type:	Article
Date Submitted by the Author:	n/a
Complete List of Authors:	Yang, Zhi; Massey University - Albany Campus, school of food and advanced technology Bhagia, Samarthya; Oak Ridge National Laboratory O'Neill, Hugh; Oak Ridge National Laboratory, Chemical Sciences Division Evans, Barbara; Oak Ridge National Laboratory, Chemical Sciences Division Ragauskas, Arthur; University of Tennessee Knoxville, Department of Chemical and Biomolecular Engineering Davison, Brian; Oak Ridge National Laboratory, Bioprocessing R & D Center Pingali, Sai Venkatesh; Oak Ridge National Laboratory, Neutron Scattering Division

Deconvoluting structures of component plant biopolymers using deuterium labeled *Brassica oleracea stems*

Zhi Yang[1,$], Samarthya Bhagia[2], Hugh O'Neill[1], Barbara R. Evans[3], Arthur Ragauskas[2,4], Brian H. Davison[2] and Sai Venkatesh Pingali[1]*

[1]Neutron Scattering Division, Oak Ridge National Laboratory, Oak Ridge TN 37831

[2]Biosciences Division, Oak Ridge National Laboratory, Oak Ridge TN 37831

[3]Chemical Sciences Division, Oak Ridge National Laboratory, Oak Ridge TN 37831

[4]Department of Chemical and Biomolecular Engineering, University of Tennessee, Knoxville, TN 37996

[$]Present address: School of Food and Advanced Technology, Massey University, Auckland 0632, New Zealand

*Email: pingalis@ornl.gov

Keywords: Partially deuterated kale; Contrast-variation SANS; FTIR; Cell wall structure; Deuterium incorporation

Abstract

Several *Brassica* species are cultivated globally for production of seed oils as food, lubricants, and increasingly biofuels. The stem and leaf residues of these herbaceous dicotyledonous crops constitute another feedstock for biofuels and other products. Plant cell walls are complex, multi-polymeric structures that consist primarily of polysaccharides and lignin. Cellulose chains coalesce to form crystalline microfibrils while the amorphous biopolymers, hemicellulose and lignin form a network structure and fill the interstitial space. Neutron scattering has been used for the structural study of the assembly and deconstruction of the plant cell walls. However, similar neutron sensitivity of the different amorphous biopolymers has made structural association to individual component biopolymers non-trivial and ambiguous. To improve the association of structural features to specific biopolymer components, partial deuteration of the plant cell wall can be employed to increase the difference in the neutron scattering length density between amorphous carbohydrate and lignin plant polymers. Vegetative stems from partially deuterated *Brassica oleracea acephala* (Kale) plants were obtained commercially and the plant cell wall structures were studied by contrast-variation small-angle neutron scattering (CV-SANS) and Fourier-transform infrared spectroscopy (FTIR). FTIR results indicated that deuterium substitution for hydrogen in the carbohydrates was higher than in lignin. By combining CV-SANS and FTIR results, the neutron scattering length density (nSLD) of the polysaccharides and lignin were determined to match nSLD of 65%:35% and 48%:52% D_2O:H_2O solvent mixtures, respectively. These nSLD values were higher than the nSLD values of polysaccharides and lignin for H_2O grown biopolymers. The nSLD increase correlates to replacing about 42.5% of hydrogens present as both C-H and O-H groups in cellulose with deuterium atoms, while only 21% for lignin. This study lays the foundation to use partially deuterated plants to deconvolute structural features of the different component biopolymers, especially cellulose, hemicellulose and lignin of the plant cell wall without introducing unintended structural modifications due to the pretreatment extraction processes.

Introduction

The unique capabilities of small-angle neutron scattering (SANS) assisted by Fourier Transform Infrared Spectroscopy (FTIR), and Nuclear Magnetic Resonance (NMR) spectroscopic techniques, and computational simulation have been applied to reveal detailed molecular structure of both natural lignocellulosic biomass[1-4] and model cellulosic composites[5, 6, 7(. In this study, these techniques are applied to examine the cell wall structure of stems of an herbaceous dicotyledonous plant stem, kale (collards), which exhibits an hierarchical structure resembling wood in vascular architecture but with lower lignification and higher pectin content.[8] Kale and other *B. oleracea spp*. are close relatives of a major oil and biomass crop, rapeseed (*Brassica napus*), which originated from a diploid fusion of *B. oleracea* and *B. rapa*[9] and the emergent biofuel crop *B. carinata*, a natural hybrid of *B. oleracea* and *B. nigra*.[10, 11] In addition to the utilization of *B. napus* seeds for food oil and biodiesel, the straw left after seed harvest is a lignocellulosic feedstock for biofuel production.

The plant cell wall is a complex material consisting of an intricate arrangement of cellulose, hemicellulose, pectin and lignin biopolymers.[12] Cell wall composition and properties of component biopolymers of kale have been reported.[13, 14] Lignin content of kale grown for culinary use (early first season harvest) was reported to be 5.6% of dry weight with high G/S ratio of 4.9.[15] Content and composition of lignin in the stems of Brassica species varies depending on age and tissue type. The lignin content of stems of two kale varieties was found to increase about two-fold from 6 months to 12 months of growth, approaching that of wood (20-30%) during the second season, while the G/S ratios increased as well.[16] As reported for the related model species Arabidopsis thaliana, flowering stems are more highly lignified than vegetative stems, with secondary xylem resembling that of wood. Increase in stem thickness correlated with decreased lignification among different cultivars. Hemicellulose was previously reported to be composed mostly of glucuronoarabinoxylan, with 20-25% xyloglucan.[13] Kale pectin was found to contain both homogalacturonan and rhamnogalacturonan I regions with molecular weights of M_w 133 kDa and M_n 17,000 by size exclusion chromatography.[14] Separation of parenchymal cells from secondary xylem cells enabled determination of their carbohydrate and lignin composition. Parenchymal cells contained higher pectin and lower lignin and lower cellulose, while the secondary xylem cells were more lignified, with lower pectin content.[13]

Deuterium labeling of spinach, carrots, and kale (collards) grown in hydroponic culture has been used to enable monitoring of metabolism of nutrients such as carotene, lutein, and tocopherol in nutritional studies.[17-19] The reported characterization of these plants has been limited to a determination of site and amount of deuterium substitution in these nutrients, in contrast to the detailed investigation of deuterium incorporation and gene expression carried out for Arabidopsis thaliana grown in 30% D_2O.[20] We have previously described the analysis of deuterium incorporation in stems of partially deuterated kale plants obtained commercially using both solution and solid phase ^1H ^2H-NMR.[21] The deuterium content of freeze-dried samples of the kale stems dissolved in ionic liquid was determined to be 33% by $^1H^2H$-NMR analysis, with higher incorporation in the carbohydrate fractions than in the lignin characteristic aromatic regions. FTIR has been utilized to estimate D incorporation in several biomass materials including deuterated bacterial cellulose,[6, 22] switchgrass,[23-25] and annual ryegrass.[26]

SANS has been used extensively to characterize plant cell wall structure.[1, 27-31] Previous applications of contrast variation small-angle neutron scattering (CV-SANS) for studies of lignocellulose and related materials had been limited to the structural characterization of deuterated bacterial cellulose and its interactions with hemicellulose[7, 22, 32, 33] as composite materials. In principle, neutron scattering can be applied to resolve structures of component biopolymers within a plant cell wall, however, from the composition and density of the component plant biopolymers such as cellulose, hemicellulose, and lignin, their neutron scattering length densities (nSLDs) to neutrons were determined to be similar. For systems in which negligible contrast exists between component biopolymers, contrast can be enhanced by utilizing methods that replace covalently bonded hydrogens (H) with deuterium (D) atoms.[34, 35] When plants are grown in media containing D_2O, the inherent variation in the cumulative impact of the D/H kinetic isotope effects in the metabolic pathways of the different plant biopolymers, can be expected to result in differential D/H substitution in these plant biopolymers. We previously demonstrated that in-vivo deuterium labeling enabled CV-SANS to distinguish the component biopolymers in tiller biomass from switchgrass, a C4 perennial prairie grass able to grow in 40-50% D_2O for several months.[4, 23, 24] In the work reported here, we now show that CV-SANS techniques can be applied similarly to a C3 annual dicot, kale, grown in a lower D_2O concentration (31% D_2O) under conditions successfully used to label many species of plants for nutritional and other studies.[17-19] The results from the commercially obtained deuterium labeled kale thus both help validate our

method and demonstrate that readily achievable levels of deuterium incorporation in plant biomass can be used to extend application of neutron scattering techniques.

Here, we report the characterization of the plant cell wall structure of partially deuterated kale stems spanning length scales from nanometer to sub-microns using CV-SANS. FTIR was included in this study as a complementary, easy to access technique, to obtain a qualitative determination of deuterium incorporation, and improve the robustness of the structural knowledge available from CV-SANS data on the plant cell wall structure. The CV-SANS method used to investigate the structure of the whole plant cell wall and the component biopolymers takes advantage of the increased contrast between component biopolymers, especially between carbohydrates (cellulose and hemicellulose) and lignin.

Materials and Methods

Deuterium labeled Brassica

Frozen vegetative stems (leaf petioles). 20 g, from partially deuterated kale (collards) plants (*Brassica oleracea* var. *acephala*, cultivar Georgia; d-kale) were obtained from a commercial source (Oak Ridge Research Reagents Inc., Oak Ridge, TN). They were stored at -80 ºC until use. According to the vendor, deuterium content was given as 31% and the plants had been produced by a published method in which seedlings were germinated and grown in vermiculite watered with normal abundance water for 14 days, then transferred to hydroponic cultivation in D_2O/H_2O mixtures.[17-19, 36] The deuterium content of α-tocopherol ($C_{29}H_{50}O_2$) in the deuterated kale grown under similar conditions was determined using mass spectroscopy to range from 9 to 13 deuterium substitutions corresponding to approximately 18-26% D.[19] Due to the limited quantity (20 g) of deuterium labeled kale samples, compositional analysis was not carried out.

Cell wall component polymers extraction

Deuterated kale stems (d-kale) were freeze-dried at -80 °C for 48 h followed by knife-milling (mini Wiley mill, Thomas Scientific Inc. Swedesboro, NJ) through ASTM standard 40-mesh (< 0.425 mm).[37] The d-kale powder underwent Soxhlet extraction with water for 6 h followed by drying in a fume hood. The powder was Soxhlet-extracted with a solvent mixture of toluene:ethanol (2:1 v/v) for 8 h followed by drying in a fume hood, and further Soxhlet-extracted with acetone for 4

h.[3] The Soxhlet-extraction with acetone removed extractives and resulted in an extractives-free d-kale.

For cellulose and hemicellulose recovery, the extractives-free d-kale powder was delignified by first peracetic acid soak (5.5 g/g biomass) at 25 °C and in a dark environment, followed by repeated centrifugation and washing at 8000 rpm in 50 mL centrifuge tubes with deionized water (Eppendorf 5804R with fixed rotor).[38] For pectin recovery, the delignified sample was treated with 50 mM ammonium oxalate at 25 °C for 24 h followed by centrifugation. The solid residue was washed thoroughly with deionized water and then treated with 1 M potassium hydroxide (KOH) + 1% sodium borohydride ($NaBH_4$) and 4 M KOH +1% $NaBH_4$ at 25 °C for 24 h each.[39] The alkaline supernatants after centrifugation were neutralized using glacial acetic acid. The ammonium oxalate, 1 M and 4 M KOH extracts were dialyzed against 10 L of deionized water for 3 days using 3500 molecular weight cut-off regenerated cellulose membranes and with water exchanged each day. The dialyzed extracts were freeze-dried to recover pectin, and 1 M and 4 M alkali-soluble hemicelluloses.[40] The yields of pectin and 4 M alkali soluble hemicellulose were very low. Therefore, only 1 M alkali-soluble hemicellulose was used for characterization. Cellulose solids after 4 M KOH treatment were washed thoroughly with deionized water by repeated centrifugation and freeze-dried.

For lignin recovery, about 100 mg of extractives-free d-kale was ball milled at 300 rpm for 8 h using six 10 mm zirconia balls with 5 min interval in a 50 mL zirconia jar in Retsch PM 100 planetary mill (Retsch USA, Newtown, PA). Since the d-kale powder was stuck on the walls of the jar, it was recovered by rinsing with deionized water followed by freeze drying. The flour was then enzymatically hydrolyzed using 150 mg total protein cocktail per gram biomass, made from mixing 100 mg Accellerase 1500, 30 mg Accellerase XY® and 20 mg Multifect pectinase (Dupont Lifesciences), in 50 mM pH 5.0 sodium citrate buffer, 0.02% sodium azide, at 50 °C, 150 rpm, for 72 h. The suspension was then centrifuged, and the remaining solids were again hydrolyzed with fresh enzyme solution for another 72 h. The suspension was then washed with water by repeated centrifugation and lignin solids were hydrolyzed with pronase (from *Streptomyces griseus*) (Sigma-Aldrich, E.C. No. 3.4.24.4) at 37 °C for 24 h at 150 rpm. The solids were washed with water by repeated centrifugation and freeze-dried at -80 °C for 24 h to recover lignin.

In all the component extraction processes described above for extractive free d-kale, extracted cellulose, hemicellulose, pectin, and lignin, h-solvents were used and therefore these samples have mostly O-H groups. Due to high solvation of hemicellulose and pectin, these plant polymers will have a lower number of O-D groups remaining. On the other hand, due to lower solvation of cellulose and lignin components, cellulose and lignin will have lower extent of O-H groups and higher extent of O-D groups.

Protiated Brassica

Commercially produced kale (collard) plants at a similar growth stage to the deuterated sample were purchased at a local grocery store and stored at -20 ºC until use. The protiated kale sample was prepared by size reduction and Soxhlet as described above for the deuterated kale plants. Compositional analysis was performed to provide an estimate on the content of the various plant biopolymers in the deuterated *Brassica* plants based on the compositional data obtained for the protiated *Brassica* sample (Table 1). The neutral sugar composition of the extractives-free protiated kale was determined by acid hydrolysis followed by analysis of the hydrolysate and sugar recovery standards by high-performance anion-exchange chromatography with pulsed amperometric detection (HPAEC-PAD) using a published method.[41] Glucose and xylose yields were used to calculate the cellulose and xylan content presented in Table 1. Extractives, ash, and lignin were determined by gravimetric analysis.

FTIR measurements

Fourier Transform InfraRed – Attenuated Total Reflection (FTIR-ATR) spectroscopy (Spectrum 100, PerkinElmer, Wellesley, MA) was carried out for extractives-free d-kale (whole biomass), cellulose, 1 M alkali-soluble hemicellulose and lignin recovered from d-kale stems in 4000–600 cm^{-1} range with a resolution of 1 cm^{-1} with 32 scans. A background scan was taken without sample. Baseline transmittance was calculated as the average transmittance for wave numbers 4000-3700 cm^{-1}, a range without IR peaks for biomass biopolymers. Minimum % transmittance was found for O-H, C-H, O-D and C-D bands between 3600-3000 cm^{-1}, 2965-2800 cm^{-1}, 2600-2340 cm^{-1}, and 2240-2030 cm^{-1}, respectively. Peak height for the band was taken as the difference

between baseline % transmittance and a minimum % transmittance of that band. Ratios were calculated from peak heights of C-D/C-H and O-D/O-H.

Small-Angle Neutron Scattering measurements.

Small-angle neutron scattering (SANS) measurements were performed at the Bio-SANS instrument at the High-Flux Isotope Reactor (HFIR), Oak Ridge National Laboratory (Oak Ridge, TN, USA).[42, 43] Two different instrument configurations were employed with the main detector at 7 m and 12 m from sample to cover a scattering vector range, $0.003 < Q$ (Å^{-1}) < 0.3 at a wavelength of 6 Å ($\Delta\lambda/\lambda$ = 13.2%), where $Q = (4\pi/\lambda)sin\theta$, and 2θ is the scattering angle and λ is the neutron wavelength. The recorded 2D neutron scattering images were azimuthally averaged and processed using MantidPlot software to obtain 1D scattering intensity profiles $I(Q)$ versus Q. The scattering data were corrected for detector dark current, pixel sensitivity, solid angle correction and sample transmission and empty titanium quartz sample cell. Absolute calibration of SANS intensity was carried out using a porous silica standard. The blank buffers containing the same D_2O percentage as the samples were measured similarly and subtracted from sample scattering as the background. To maximize exchange of O-H to O-D of deuterated kale and its cellulose extract samples from the deuterium in the solvent prior to SANS measurement, the deuterated kale stalks and its cellulose extracts were soaked in D_2O/H_2O solvent mixtures for at least 24 h. This involved two 2 h soaks with fresh solvent mixtures followed by an overnight soak followed by the last change to a fresh solvent mixture 1-2 h before samples were loaded into titanium cells (for deuterated kale stems, vertically aligned) and filled with equilibration solvents to ensure no bubbles were present in the cells before SANS measurements.

SANS data of deuterated kale stems and its cellulose extracts soaked in 0% D_2O was analyzed using the IRENA SAS macro implemented in Igor Pro software (Wavemetrics, USA).[44] The Unified Fit approach was employed to deconvolute structural features spanning multiple lengths scales; the scattering exhibited by each structural level is the combination of a Guinier exponential-form and a structurally limited power-law tail. The expression is:

$$I(Q) = \sum_{i=1}^{n} G_i \exp\left(\frac{-Q^2 R_{gi}^2}{3}\right) + B_i \exp\left(\frac{-Q^2 R_{g(i+1)}^2}{3}\right)\left[\frac{(\mathrm{erf}(QR_{gi}/\sqrt{6}))^3}{Q}\right]^{Pi} \quad (1)$$

where n is the number of the structural level, G is exponential pre-factor and R_g is the radius of gyration. B and P are the pre-factor and the exponent of the power-law function, respectively.[45, 46] All reported error bars in this manuscript were obtained by performing error bar analysis as part of the fitting routine in the IRENA[44] fitting package by using the feature '*analyze uncertainty*'.

Results

FTIR Estimation of Deuterium Incorporation:

FTIR measurements were performed on partially deuterated whole kale stem samples as well as on the extracted plant biopolymers cellulose, hemicellulose, and lignin. In addition to the usual C-H and O-H stretching bands, all the FTIR patterns also showed the presence of a C-D (2300-2000 cm^{-1}) and O-D (2500 cm^{-1}) stretching band indicating that deuterium atoms were successfully incorporated into all the component biopolymers of the partially deuterated kale stem sample (Figure 1; Table 2). An exception was observed for extracted hemicellulose sample; the O-D band was absent. Cellulose and hemicellulose have exchangeable hydrogen atoms as O-H groups on the 2nd, 3rd, and 6th carbon atoms of the glucose ring. Similarly, lignin also has O-H groups on the 3rd carbon of the phenolic ring and the terminal carbon of the tail.[47] The higher hydrophilic nature of hemicellulose makes its O-D groups highly susceptible to exchange to O-H in h-solvents which was used for extraction and lyophilization to prepare samples for FTIR measurement. Consequently, FTIR measurement of extracted hemicellulose does not detect an O-D peak in the FTIR spectrum. The peak emissions of the stretching bands of C-D is different from C-H (3000-2800 vs. 2300-2000 cm^{-1}) making it easy to distinguish between them and similarly for O-D to O-H stretching bands (2500 vs. 3400 cm^{-1}). This difference is used to qualitatively determine deuteration extent and improve data interpretation of CV-SANS. Unlike C-H and C-D groups, the equilibrium ratio of O-H/O-D in the samples is highly dependent on the O-H/O-D ratio of the incubating solvent. All FTIR samples were soaked in 100% H_2O solvents implying all solvent accessible O-D groups within the cell wall will have exchanged back to O-H groups. On the other hand, CV-SANS samples were soaked in solvents with increasing amounts of O-D groups (0 to 100% D_2O) implying increasing extent of O-H groups will exchange to O-D, increasing the extent of O-D groups in CV-SANS samples compared to FTIR samples. Due to this inconsistency in the extent of O-D groups between FTIR and CV-SANS samples, only the ratios of non-exchangeable hydrogens (C-H/C-D) obtained by FTIR analysis were used for combining with CV-SANS data.

CV-SANS Estimation of Deuterium Incorporation:

Partially deuterated kale (d-kale) stems were studied using CV-SANS to determine the structure of the plant biopolymers, cellulose, hemicellulose, and lignin in the cell walls. Interestingly, FTIR measurements showed a qualitative difference of D incorporation into carbohydrate and the lignin biopolymers. This differential incorporation of D affects the neutron SLD of these biopolymers beneficially by increasing their contrast and ability to distinguish between them. The scattering intensity profiles of whole d-kale stems and cellulose extracts of the d-kale stems in a series of D_2O/H_2O aqueous solvents (0 to 100% D_2O) are plotted in Figures 2A and 2B, respectively. Previously, deuterated kale stems dissolved in ionic liquid with d/h-TFA internal standards were found by $^1H^2H$-NMR to have 33% D substitution in the range assigned to carbohydrates and aliphatic groups of lignin,[21] while no D substitution was detected in the aromatic region. Similar results were obtained for annual ryegrass cultivated in 50% D_2O.[26] At this level of D incorporation, cellulose, and lignin neutron SLD is much closer to 100% D_2O solvent than 0% D_2O. Consistent to this expectation, whole d-kale stems, and cellulose extracts in 0% D_2O solvent produced maximum scattering intensities for the entire measured Q-range indicating these partially deuterated plant samples had maximum neutron contrast in 0% D_2O solvent. Therefore, SANS scattering data of d-kale stem samples in 0% D_2O solvent was used for deconvoluting the hierarchical structure of the plant cell wall. Unified fit approach with three structural levels was employed; Deconvoluted profiles for each level are shown in Figures 2C and 2D and the fit parameters (power-law exponents, P, and the radius of gyration, R_g) are summarized in Table 3. The application of contrast variation study here relies on the condition that the dominant scattering feature in the high-Q region is from cellulose microfibrils and is approximated as a two-phase system of cellulose microfibril and water. Similarly, in the low-Q region, the approximated two-phase system is cell wall and water filled lumens in deuterated kale sample or cellulose macrofibrils and water in extracted cellulose. These two systems behave independently due to their significantly different length scales of 20-40 Å for the cellulose microfibril feature and 0.1-0.2 microns for the surface characteristics of the cell wall lumen in d-kale sample or cellulose macrofibrils in the extracted cellulose sample.

Plant cell wall hierarchical structure: The shoulder feature observed in the high-Q region, $0.05 < Q$ (Å^{-1}) < 0.4, of partially deuterated kale stem (Figure 2C) and its extracted cellulose samples (Figure 2D) was modeled to a particle size and ascribed to the cross-sectional R_g of the cellulose microfibril.[27, 47, 48] The measured values are 15 ± 1 Å and 24 ± 3 Å, respectively. The cross-sectional R_g for partially deuterated kale stem sample is slightly higher than reported R_g for native switchgrass[27] and poplar[1] (~9.0 Å) and close to microcrystalline cellulose Avicel PH-105[49] (18.5 ± 0.5 Å). On the other hand, the cross-sectional R_g for extracted cellulose was much larger than even microcrystalline cellulose Avicel PH-105 indicating that the extraction process has promoted the coalescence of neighboring crystalline cellulose microfibrils. The behavior of increased cellulose microfibril R_g has been reported for native switchgrass and its extracted cellulose samples too, R_g ~ 8.7 ± 0.6 Å and ~13.6 ± 1.0 Å, respectively,[49] even though the absolute values are lower.

In the mid-Q region, $0.006 < Q$ (Å^{-1}) < 0.05, the scattering intensity demonstrated a power-law decay behavior (Q^{-P}); $P = 2.10 \pm 0.04$ was observed for length scales 125-1050 Å ($=2\pi/Q$), for partially deuterated kale stem sample soaked in 0% D_2O solvent indicating that the scattering characteristics refer to the spatial conformation of the biopolymers- amorphous polysaccharides and possibly lignin too.[27] A power-law exponent of 2.1 for a system of biopolymers indicates that the amorphous polymers responsible for this feature exhibits random flexible conformation. Also, this characteristic can be observed by these amorphous polymer chains being either linear and entangled or mildly branched. This interpretation is consistent with hemicellulose, pectin and lignin biopolymers. On the other hand, removal of the amorphous plant polymers as in the extracted cellulose sample, showed the coalescence or aggregation of microfibrils to form macrofibrils with R_g of 190 ± 28 Å. And a mass fractal exponent of 2.50 ± 0.05 implies the organization of the cellulose microfibrils in the aggregate are dense and entangled. The observation of dense entangled aggregates in the mid-Q region combined with cellulose microfibril coalescence in the high-Q region, show an increased propensity for cellulose structure to aggregate with removal of hemicellulose, pectin, and lignin.

The power-law decay behavior extended into the low-Q region, $0.003 < Q$ (Å^{-1}) < 0.007, for both samples. However, due to the limited range of Q available for fitting (0.003 - 0.007 Å^{-1}), the exponent was only qualitatively interpreted. A clear cross-over to a steeper slope ($P > 3.0$) was

observed around $Q \sim 0.007$ Å^{-1} for partially deuterated kale stem sample, while for extracted cellulose sample, the same mid-Q slope propagated into the low-Q region ($P < 3.0$). This observation indicated that only surface characteristics of the intact micron-sized structural features (> ~0.1 μm; $=2\pi/Q_{max}$; $Q_{max} \sim 0.007$ Å^{-1}) were observed for partially deuterated kale stem sample, for example, the surface characteristics of the cell wall lumen. In contrast, only bulk characteristics was observed for extracted cellulose sample. The loss of surface morphology feature in the low-Q region for extracted cellulose sample implied that the extraction process disrupted the cell lumen structure by the removal of the amorphous biopolymers. The loss of the cell wall lumen structure combined with the pronounced coalescence of cellulose microfibrils to form macrofibrils make the cellulose macrofibril feature become the most visible scattering signal in the low-Q region.

Determination of contrast match point: Figure 2A shows the SANS profiles of partially deuterated kale stem samples in a series of H_2O/D_2O solvent mixtures- 0, 20, 40, 55, 75 and 100% D_2O. Each cell contained equal number of d-kale stem material in H_2O/D_2O solvent. The square-root of the scattering intensity at a fixed Q-value was plotted as a function of solvent $\%D_2O$. A linear relation was observed and the intersect with x-axis was used to determine the contrast matched solvent mixture (see Figures 2A and 2B insets). For example, at Q=0.05 Å^{-1} the contrast matched solvent ratio is 63.7% D_2O for partially d-kale stem sample and 69.4% D_2O for its extracted cellulose sample. Further, to calculate nSLD (in units of 10^{-6} Å^{-2}) from the $\%D_2O$ value determined, the equation $nSLD = -0.56 + 6.92\ f_{D_2O}$, where f_{D_2O} is the fraction of D_2O of the contrast matched solvent was used. For example, if the contrast matched solvent is 70% D_2O, then $f_{D_2O} = 0.7$ in the equation and $nSLD = 4.28 \times 10^{-6}$ Å^{-2}. The coefficients used were obtained from nSLDs of 100% H_2O (-0.56×10^{-6} Å^{-2}) and 100% D_2O (6.36×10^{-6} Å^{-2}).

Contrast match point of the different component biopolymers: The method of determining contrast-matched solvent for a single Q-value, as detailed in the previous paragraph, was applied to several selected Q-values that spanned the entire Q-range of the measured SANS profile (Figure 3). Based on the component biopolymers responsible for the structural features in the different Q-regions, the Q-resolved contrast matching solvents obtained were used to determine the extent of D/H substitution to the different component biopolymers. The concept of 'Q-dependence of scattering length density' has been reported in literature on the structural study of *E.coli*[50, 51] and a

computation effort for a simpler system of protein in solution[52]. A similar approach was applied in this study and more details is provided in supplementary information under '*Q*-dependence of scattering length density'. With the scattering signal in the high-*Q* region (> 0.07 $Å^{-1}$) dominated by the cellulose microfibril structure, the contrast matched solvent for partially deuterated cellulose in d-kale stem sample was measured to be ~65.0 ± 2.5% D_2O solvent (nSLD = 3.94 ± 0.17 x 10^{-6} $Å^{-2}$). For partially deuterated cellulose in the extracted cellulose sample, the contrast matched solvent is slightly higher at 69.0 ± 2.5% D_2O solvent (nSLD = 4.21 ± 0.17 x 10^{-6} $Å^{-2}$) consistent with the removal of hemicellulose because hemicellulose has a lower nSLD than cellulose. In the low-*Q* region (0.004-0.03 $Å^{-1}$) *Q*-resolved contrast matched solvent was slightly higher at ~72.5 ± 1.0% D_2O solvent (nSLD = 4.46 ± 0.07 x 10^{-6} $Å^{-2}$) for the extracted cellulose sample. An overall contrast matched solvent of 65-75% D_2O solvent implies that all structural features of the extracted cellulose sample, high- and low-*Q,* are associated with the cellulose component of the plant biopolymers. Further, a higher contrast match point of +3.5% D_2O in the region of the macrofibril feature ($Q < 0.03$ $Å^{-1}$) can be explained as the average nSLD of different populations of cellulose microfibrils and water (or D_2O) filled spaces. The volume fraction of solvent molecules necessary for such an increase in the nSLD is ~11%.

In contrast, d-kale stem sample showed a gradual reduction in the D_2O% of the contrast matched solvent from $Q \sim 0.04$ $Å^{-1}$ to $Q \sim 0.015$ $Å^{-1}$ and eventually levelled at ~48% D_2O in the low-*Q* region, 0.003 – 0.01 $Å^{-1}$. This indicated that a plant biopolymer with much lower nSLD than partially deuterated cellulose was responsible for the scattering signal in the low-*Q* region. Since, surface characteristics of large structures (< 0.1 μm) in the plant cell wall is observed in the low-*Q* region, the contrast match point of ~48% D_2O was associated with one or more of the amorphous plant biopolymers- hemicellulose, pectin, and lignin, present on the surface of these large structures. Applying qualitative estimation, hydrophilic polysaccharides hemicellulose, and pectin biopolymers are expected to follow or do better than cellulose component in the extent of O-H exchange to O-D due to better solvation and with a density that is similar to cellulose, nSLD will be close to cellulose (~65% D_2O). On the other hand, hydrophobic lignin biopolymer will have a low degree of O-H exchanged to O-D due to a combined effect of low water penetration and a low degree of deuteration of the non-exchangeable as obtained from FTIR. Therefore, the nSLD of lignin biopolymer will only increase slightly. This implies that the contrast match point of ~48%

D_2O observed in the low-Q region is mostly associated with features that contain partially deuterated lignin biopolymer. With lignin found to concentrate within 1-2 microns on the surface of the cell wall lumen,[53] it implies that the low-Q surface scattering for the d-kale stem sample is of the cell wall lumen and not aggregates of cellulose microfibrils.

Quantification of O-H to O-D exchange:

FTIR analysis revealed ~2.22 of 7 C-H groups were replaced by C-D in d-kale cellulose and ~0.59 O-H groups were replaced by O-D. Together, the calculated nSLD from FTIR measurements of the contrast matched solvent is 57% D_2O which is lower than the SANS measured contrast matched solvent of 65% and 69% D_2O for d-kale stem and extracted d-kale cellulose samples, respectively. This difference is attributed to the higher extent of O-H groups exchanged to O-D that occurred for the SANS samples during sample soaking process employed for contrast variation SANS measurements. The soaking process has been described in the 'Small-Angle Neutron Scattering Measurement' sub-topic of 'Methods and Materials' section. Furthermore, samples for FTIR measurements were in hydrogenated solvents which will have facilitated re-exchange of O-D groups back to O-H groups resulting in increased O-H groups. Using the number of C-D groups measured by FTIR analysis, a nSLD of 65% D_2O as measured by SANS indicated approximately 1.54 of 3.0 O-H groups were replaced by O-D for the d-kale stem sample, while a nSLD of 69% D_2O for d-kale cellulose sample implied approximately 2.03 of 3.0 O-H groups were replaced. The d-kale cellulose sample exhibited a slightly higher degree of solvent penetration resulting in a higher degree of O-H group exchange to O-D group. In summary, SANS results indicated that approximately 4.25 deuterium atoms were present in the form of C-D/O-D groups out of 10 total groups in d-kale cellulose sample and approximately 3.76 of 10 for d-kale stem sample.

The major type of hemicellulose in the kale plant cell wall is glucuronoarabinoxylan with a wide variation in the degree of branching and substitution of acetyl and glucuronic acid groups.[13] These hemicelluloses are amorphous and hydrophilic and mainly contain hexoses (glucose) and pentoses (arabinose and xylose). Irrespective, hemicelluloses have 3 O-H hydrogens of the 8 or 10 available in total and being hydrophilic, they are freely available for exchange with solvent and therefore, it is safe to assume that at least 50% of all the available O-H groups in the system have exchanged to O-D. Further, FTIR results shows that 1.5 C-H hydrogen of the 10 (hexoses) or 1.07 C-H

hydrogens of 8 (pentoses) have been replaced by C-D. With a density of 1.5 g/cm^3 and combining all hydrogen replacements C-H and O-H, the contrast match point of the hemicelluloses is greater than 59% D_2O. This implies the contrast matched solvent mixture of 48% D_2O measured for the low-*Q* region of the data is not from a feature that predominantly has hemicellulose on its surface.

Lignin is composed of three monomers sinapyl, S, coniferyl, G, and p-coumaryl, H, with the amounts of each monomer dependent on plant type and tissue. In addition, depending on the composition of the lignin molecule, its density varies between 1.35 to 1.50 g/cm^3.[54] With such a wide range in the lignin polymer's monomer composition and density, it is difficult to precisely determine nSLD of a lignin molecule. However, to estimate an average nSLD of lignin, the middle-sized monomer, coniferyl monomer G, was selected with an approximate density of 1.35 g/cm^3 and 2.05 C-D groups (of 10) as determined by FTIR was used. The calculated nSLD for d-lignin was then 47% D_2O, which agrees with the contrast matched solvent mixture of 48% D_2O obtained by SANS measurement in the low-*Q* region. This implies that on the average, most exchangeable hydrogens (O-H groups) at any given instant were mostly not exchanged to deuteriums (O-D groups) for the lignin molecule. On the other hand, the contrast matched solvent mixture for d-hemicellulose, detailed in the earlier paragraph, is much higher than 48% D_2O, adding to the interpretation that low-*Q* feature is most probably due to lignin molecules on the surface of the micron-sized structures contributing to the scattering signal in the low-*Q* region of the SANS profile.

Discussion

SANS and FTIR results showed preferential incorporation of deuterium into cellulose consistent with previous NMR findings on similar samples.[21] Deuterium incorporation into C-H groups of cellulose, hemicellulose, and lignin plant biopolymers obtained by FTIR were 32% (2.22/7.0), 21% (1.5/7.0 for hexoses or 1.07/5.00 for pentoses) and 21% (2.05/10.00), respectively. The uneven distribution of deuterium incorporation among the different component biopolymers of the plant cell wall can be attributed to the inherent variation in the metabolic pathways of the different plant biopolymers during hydroponic cultivation. Unfortunately, the detailed metabolic pathways of plant growth particularly in deuterium-enriched media are largely unknown. Considering photosynthesis is an extremely complicated biological process, other factors including the

differences in hydrophobicity and relative development/growth rates of cellulose and lignin may also result in differential D incorporation. Further studies involving monitoring the D incorporation into the cell wall component biopolymers as well as cell wall compositional changes at different growth stages could be helpful to reveal the different extent of D incorporation and the underlying mechanism in more detail. The ability to distinguish molecular structural features in the plant cell walls of plants grown in the typically non-inhibitory level of 31% D_2O will enable extension of CV-SANS to study their root systems, which play important roles in absorption and transportation of nutrients and water from soil as well as response to various abiotic stresses.[55]

To obtain the degree of D incorporation in different plant cell wall component biopolymers through CV-SANS measurements, the knowledge regarding the extent of O-H exchange to O-D was required. The distribution of hydroxyl groups in the interior and on the surface of the component biopolymers particularly for hemicellulose, and lignin, which subsequently influences their accessibility to solvents and the extent of O-H exchange to O-D was estimated. Furthermore, beside lignin, cellulose, and hemicellulose, kale has around 10-20% and 30-40% pectin in the total cell wall material of its secondary xylem and parenchyma cells, respectively.[8, 13] Similar to hemicellulose, pectin exhibits a branched structure[56] and has a similar density, so the neutron SLD of pectin was estimated to be similar to hemicellulose which implies that pectin could not be responsible for low-*Q* structural feature. Furthermore, computational simulations on the behaviors of the component biopolymers in different D_2O:H_2O solvents could also be used to validate these assumptions by imposing more constraints.[48, 57] Localization and quantification of D incorporation in the component biopolymers cellulose, hemicellulose, pectin, and lignin with $^1H^2H$-NMR and mass spectroscopy would provide more specific information on their interactions in the cell wall.[23, 24] By combining these experimental methods (FTIR, NMR, and neutron scattering) and computational simulations, the hierarchical plant cell wall structures and D incorporation can be characterized and determined in greater detail to that presented in this work.[58]

The detailed, in-depth analysis of the hierarchical structure of plant lignocellulosic biomass using neutron scattering has been hampered by the existence of marginal neutron scattering contrast among the different cell wall biopolymer components. However, hydroponic growth of kale plants in 31% deuterated media to produce d-kale sample with variable deuterium incorporation,

enhanced the contrast between lignin and cellulose. Therefore, structural studies of the different biopolymer components in the complex plant cell wall can now be performed in its native state without the need to deconstruct and fractionate the different plant cell wall biopolymer components. This is extremely important since many unintended irreversible structural changes occur to the component biopolymers as well as to the entire cell wall architecture, when subjected to extraction and sample preparation processes.[59, 60] For example, increase of cellulose microfibril size and appearance of a larger aggregate (R_g~190 Å) has been observed in the cellulose extracts compared to those of native kale stem (Figure 2). To alleviate the issues of unintended modifications due to extraction processes, partially deuterated kale with the increased contrast between cellulose and lignin makes as an excellent model system to study the effect of pretreatment and improve our chance of resolving the contribution from different biopolymer components. This will help us understand the underlying structural complexity of plant recalcitrance toward cell wall deconstruction for biofuel production. The deconvolution approach employed here have already been demonstrated for switchgrass and can be used to determine the extent of deuterium incorporation for other biofuel-relevant plant systems such as poplar.[4] Since many plant species have been reported to grow close to normal in 30% D_2O, the ability to distinguish the component biopolymers by CV-SANS approach at these deuteration levels will extend its experimental application.[23] Finally, the use of deuterated biomass in neutron scattering studies requires both the extent of D incorporation as well as an examination of deuteration on any potential structural alternations of cell wall component biopolymers. The latter will be conducted in future studies following similar procedures that have been developed for deuterated switchgrass.[3, 25, 39]

Conclusions

Partially deuterated kale plants produced by hydroponic cultivation in 31% deuterium media had partial deuteration of the stems. Deuterium (D) incorporation was not uniform and homogeneous among the different cell wall component biopolymers. SANS determined the total deuterium incorporation for cellulose and lignin component biopolymers and by using FTIR determined deuterium atom incorporation into C-D groups, the extent of hydroxyl O-H exchange to O-D in the cell wall component biopolymers was also determined and established a comprehensive picture of the deuterium incorporation scheme.

The cross-sectional dimension of the cellulose microfibrils observed in high-Q region ($Q > 0.08$ Å^{-1}) contrast matched with 65% and 69% D_2O solvent for d-kale and extracted d-kale cellulose stem samples, respectively. The difference was associated to the differing amount of solvent penetration that afforded a difference on the average extent of O-H exchange to O-D. Consistent with the hydrophobic characteristic of lignin biopolymer, lignin indicated minimal extent of O-H exchange to O-D. Deuterium incorporation in the cellulose component of the deuterated kale stem was consistent with its cellulose extracts, nSLD = 4.21 ± 0.17 x 10^{-6} Å^{-2} (~69.0 ± 2.5 %D_2O) over the whole Q range, which is comparable to nSLD = 3.94 ± 0.17 x 10^{-6} Å^{-2} (65.0 ± 2.5 %D_2O) solvent obtained for the cellulose component in the deuterated kale stem. In the low-Q region, the large-scale cell wall surface features responsible for the power law decay (~Q^{-4}) show a neutron sensitivity that matches 48% D_2O solvent. To obtain an overall nSLD that is lower than cellulose, the SLDs of other cell wall component biopolymers like lignin and hemicellulose needs to be lower to off-set the high nSLD of cellulose within the cell wall. With evidence that lignin is located on the surface of the cell wall, 1.5 to 1.75 of the total 10 available covalently bonded H atoms need to be replaced by D atoms. This number is identified as 2.05 in the lignin extracts by FTIR. Finally, this study revealed the hierarchical structures of deuterated kale stems and varying amounts of deuterium incorporation in the different cell wall component biopolymers. These discoveries offer valuable insights to understanding the in vivo plant deuteration process. Moreover, it provides a methodology to study the biopolymer structures of lignocellulosic biomass and their response to various treatments that may be employed in biofuel production.

Acknowledgments

This research was supported by the U.S. Department of Energy, Office of Science, through the Genomic Science Program, Office of Biological and Environmental Research, under Contract FWP ERKP752. The research at Oak Ridge National Laboratory's Center for Structural Molecular Biology (CSMB) was supported by the U.S. Department of Energy, Office of Science, through the Office of Biological and Environmental Research under Contract FWP ERKP291, using facilities supported by the Office of Basic Energy Research, U.S. Department of Energy.

Supporting Information

A figure with a paragraph of detailed explanation on '*Q*-dependence on scattering length density' is provided.

Author Contributions

Z.Y. and B.R.E. prepared samples for SANS measurements; Z.Y. and S.V.P. performed SANS measurements and data analysis and H.'O'N. provided critical feedback during analysis; S.B. prepared samples and performed FTIR and compositional analysis with guidance from A.J.R; S.V.P., H.O'N., and B.H.D. directed research; S.V.P., Z.Y., and B.R.E. wrote the manuscript with input from all co-authors. All authors had the opportunity to read and comment on the manuscript.

References

(1) Pingali, S. V.; Urban, V. S.; Heller, W. T.; McGaughey, J.; O'Neill, H.; Foston, M. B.; Li, H.; Wyman, C. E.; Myles, D. A.; Langan, P.; et al. Understanding Multiscale Structural Changes During Dilute Acid Pretreatment of Switchgrass and Poplar. *ACS Sustainable Chemistry & Engineering* **2017**, *5* (1), 426-435. DOI: 10.1021/acssuschemeng.6b01803.

(2) Petridis, L.; Pingali, S. V.; Urban, V.; Heller, W. T.; O'Neill, H. M.; Foston, M.; Ragauskas, A.; Smith, J. C. Self-similar multiscale structure of lignin revealed by neutron scattering and molecular dynamics simulation. *Physical Review E* **2011**, *83* (6 Pt 1), 061911. DOI: 10.1103/PhysRevE.83.061911.

(3) Bhagia, S.; Meng, X.; Evans, B. R.; Dunlap, J. R.; Bali, G.; Chen, J.; Reeves, K. S.; Ho, H. C.; Davison, B. H.; Pu, Y.; et al. Ultrastructure and Enzymatic Hydrolysis of Deuterated Switchgrass. *Scientific Reports* **2018**, *8* (1), 13226. DOI: 10.1038/s41598-018-31269-w.

(4) Evans, B. R.; Pingali, S. V.; Bhagia, S.; O'Neill, H. M.; Ragauskas, A. J. Structural Studies of Deuterium-Labeled Switchgrass Biomass. In *Understanding Lignocellulose: Synergistic Computational and Analytic Methods*, Smith, M. D. Ed.; ACS Symposium Series, 2019; pp 17-32.

(5) Martinez-Sanz, M.; Gidley, M. J.; Gilbert, E. P. Hierarchical architecture of bacterial cellulose and composite plant cell wall polysaccharide hydrogels using small angle neutron scattering. *Soft Matter* **2016**, *12* (5), 1534-1549. DOI: 10.1039/c5sm02085a.

(6) Bali, G.; Foston, M. B.; O'Neill, H. M.; Evans, B. R.; He, J.; Ragauskas, A. J. The effect of deuteration on the structure of bacterial cellulose. *Carbohydrate Research* **2013**, *374*, 82-88. DOI: 10.1016/j.carres.2013.04.009.

(7) Shah, R.; Huang, S.; Pingali, S. V.; Sawada, D.; Pu, Y.; Rodriguez, M., Jr.; Ragauskas, A. J.; Kim, S. H.; Evans, B. R.; Davison, B. H.; et al. Hemicellulose-Cellulose Composites Reveal Differences in

Cellulose Organization after Dilute Acid Pretreatment. *Biomacromolecules* **2019**, *20* (2), 893-903. DOI: 10.1021/acs.biomac.8b01511.

(8) Wilson, W. D.; Jarvis, M. C.; Duncan, H. J. In-vitro digestibility of kale (Brassica oleracea) secondary xylem and parenchyma cell walls and their polysaccharide components. *Journal of the Science of Food and Agriculture* **1989**, *48* (1), 9-14. DOI: 10.1002/jsfa.2740480103.

(9) Snowdon, R., Lühs, W., Friedt, W. . *Oilseeds. Genome Mapping and Molecular Breeding in Plants*; Springer-Verlag Berlin Heidelberg, 2007. DOI: 10.1007/978-3-540-34388-2_2.

(10) Hossain, Z.; Johnson, E. N.; Wang, L.; Blackshaw, R. E.; Cutforth, H.; Gan, Y. Plant establishment, yield and yield components of Brassicaceae oilseeds as potential biofuel feedstock. *Industrial Crops and Products* **2019**, *141*, 111800. DOI: 10.1016/j.indcrop.2019.111800.

(11) Kumar, S.; Seepaul, R.; Mulvaney, M. J.; Colvin, B.; George, S.; Marois, J. J.; Bennett, R.; Leon, R.; Wright, D. L.; Small, I. M. Brassica carinata genotypes demonstrate potential as a winter biofuel crop in South East United States. *Industrial Crops and Products* **2020**, *150*, 112353. DOI: 10.1016/j.indcrop.2020.112353.

(12) McCann, M. C.; Knox, J. P. *Plant Cell Wall Biology: Polysaccharides in Architectural and Developmental Contexts.*; 2018. DOI: 10.1002/9781119312994.apr0443.

(13) Wilson, W. D.; Barwick, J. M.; Lomax, J. A.; Jarvis, M. C.; Duncan, H. J. Lignified and Non-Lignified Cell-Walls from Kale. *Plant Science* **1988**, *57* (1), 83-90. DOI: 10.1016/0168-9452(88)90144-6.

(14) Samuelsen, A. B.; Westereng, B.; Yousif, O.; Holtekjolen, A. K.; Michaelsen, T. E.; Knutsen, S. H. Structural features and complement-fixing activity of pectin from three Brassica oleracea varieties: white cabbage, kale, and red kale. *Biomacromolecules* **2007**, *8* (2), 644-649. DOI: 10.1021/bm060896l.

(15) Bunzel, M.; Seiler, A.; Steinhart, H. Characterization of dietary fiber lignins from fruits and vegetables using the DFRC method. *Journal of Agricultural and Food Chemistry* **2005**, *53* (24), 9553-9559. DOI: 10.1021/jf0520037.

(16) Evans, B. W.; Snape, C. E.; Jarvis, M. C. Lignification in relation to the biennial growth habit in brassicas. *Phytochemistry* **2003**, *63* (7), 765-769. DOI: 10.1016/s0031-9422(03)00327-3.

(17) Grusak, M. A. Plant foods as sources of pro-vitamin A: application of a stable isotope approach to determine vitamin A activity. *Trees for Life Journal* **2005**, *1:4*.

(18) Putzbach, K.; Krucker, M.; Albert, K.; Grusak, M. A.; Tang, G.; Dolnikowski, G. G. Structure determination of partially deuterated carotenoids from intrinsically labeled vegetables by HPLC-MS and 1H NMR. *Journal of Agricultural and Food Chemistry* **2005**, *53* (3), 671-677. DOI: 10.1021/jf0487506.

(19) Traber, M. G.; Leonard, S. W.; Bobe, G.; Fu, X.; Saltzman, E.; Grusak, M. A.; Booth, S. L. alpha-Tocopherol disappearance rates from plasma depend on lipid concentrations: studies using deuterium-labeled collard greens in younger and older adults. *The American Journal of Clinical Nutrition* **2015**, *101* (4), 752-759. DOI: 10.3945/ajcn.114.100966.

(20) Yang, X. Y.; Chen, W. P.; Rendahl, A. K.; Hegeman, A. D.; Gray, W. M.; Cohen, J. D. Measuring the turnover rates of Arabidopsis proteins using deuterium oxide: an auxin signaling case study. *Plant Journal* **2010**, *63* (4), 680-695. DOI: 10.1111/j.1365-313X.2010.04266.x.

(21) Foston, M. B.; McGaughey, J.; O'Neill, H.; Evans, B. R.; Ragauskas, A. Deuterium incorporation in biomass cell wall components by NMR analysis. *Analyst* **2012**, *137* (5), 1090-1093. DOI: 10.1039/c2an16025k.

(22) He, J. H.; Pingali, S. V.; Chundawat, S. P. S.; Pack, A.; Jones, A. D.; Langan, P.; Davison, B. H.; Urban, V.; Evans, B.; O'Neill, H. Controlled incorporation of deuterium into bacterial cellulose. *Cellulose* **2014**, *21* (2), 927-936. DOI: 10.1007/s10570-013-0067-4.

(23) Evans, B. R.; Shah, R. Chapter Ten - Development of Approaches for Deuterium Incorporation in Plants. In *Methods in Enzymology*, Kelman, Z. Ed.; Vol. 565; Academic Press, 2015; pp 213-243.

(24) Evans, B. R.; Bali, G.; Foston, M.; Ragauskas, A. J.; O'Neill, H. M.; Shah, R.; McGaughey, J.; Reeves, D.; Rempe, C. S.; Davison, B. H. Production of deuterated switchgrass by hydroponic cultivation. *Planta* **2015**, *242* (1), 215-222. DOI: 10.1007/s00425-015-2298-0.

(25) Meng, X. Z.; Evans, B. R.; Yoo, C. G.; Pu, Y. Q.; Davison, B. H.; Ragauskas, A. J. Effect of in Vivo Deuteration on Structure of Switchgrass Lignin. *ACS Sustainable Chemistry & Engineering* **2017**, *5* (9), 8004-8010. DOI: 10.1021/acssuschemeng.7b01527.

(26) Evans, B. R.; Bali, G.; Reeves, D. T.; O'Neill, H. M.; Sun, Q.; Shah, R.; Ragauskas, A. J. Effect of D2O on growth properties and chemical structure of annual ryegrass (Lolium multiflorum). *Journal of Agricultural and Food Chemistry* **2014**, *62* (12), 2595-2604. DOI: 10.1021/jf4055566.

(27) Pingali, S. V.; Urban, V. S.; Heller, W. T.; McGaughey, J.; O'Neill, H.; Foston, M.; Myles, D. A.; Ragauskas, A.; Evans, B. R. Breakdown of cell wall nanostructure in dilute acid pretreated biomass. *Biomacromolecules* **2010**, *11* (9), 2329-2335. DOI: 10.1021/bm100455h.

(28) Plaza, N. Z.; Pingali, S. V.; Qian, S.; Heller, W. T.; Jakes, J. E. Informing the improvement of forest products durability using small angle neutron scattering. *Cellulose* **2016**, *23* (3), 1593-1607. DOI: 10.1007/s10570-016-0933-y.

(29) Sawada, D.; Kalluri, U. C.; O'Neill, H.; Urban, V.; Langan, P.; Davison, B.; Pingali, S. V. Tension wood structure and morphology conducive for better enzymatic digestion. *Biotechnology for Biofuels* **2018**, *11*, 44. DOI: 10.1186/s13068-018-1043-x.

(30) Pingali, S. V.; Smith, M. D.; Liu, S. H.; Rawal, T. B.; Pu, Y.; Shah, R.; Evans, B. R.; Urban, V. S.; Davison, B. H.; Cai, C. M.; et al. Deconstruction of biomass enabled by local demixing of cosolvents at cellulose and lignin surfaces. *Proceedings of the National Academy of Sciences of the United States of America* **2020**, *117* (29), 16776-16781. DOI: 10.1073/pnas.1922883117.

(31) Zhu, Y.; Plaza, N.; Kojima, Y.; Yoshida, M.; Zhang, J.; Jellison, J.; Pingali, S. V.; O'Neill, H.; Goodell, B. Nanostructural Analysis of Enzymatic and Non-enzymatic Brown Rot Fungal Deconstruction of the Lignocellulose Cell Wall†. *Frontiers in Microbiology* **2020**, *11*. DOI: 10.3389/fmicb.2020.01389.

(32) Martínez-Sanz, M.; Lopez-Sanchez, P.; Gidley, M. J.; Gilbert, E. P. Evidence for differential interaction mechanism of plant cell wall matrix polysaccharides in hierarchically-structured bacterial cellulose. *Cellulose* **2015**, *22* (3), 1541-1563. DOI: 10.1007/s10570-015-0614-2.

(33) Martínez-Sanz, M.; Mikkelsen, D.; Flanagan, B. M.; Gidley, M. J.; Gilbert, E. P. Multi-scale characterisation of deuterated cellulose composite hydrogels reveals evidence for different interaction

mechanisms with arabinoxylan, mixed-linkage glucan and xyloglucan. *Polymer* **2017**, *124*, 1-11. DOI: 10.1016/j.polymer.2017.07.036.

(34) O'Neill, H.; Shah, R.; Evans, B. R.; He, J.; Pingali, S. V.; Chundawat, S. P. S.; Jones, A. D.; Langan, P.; Davison, B. H.; Urban, V. Chapter Six - Production of Bacterial Cellulose with Controlled Deuterium–Hydrogen Substitution for Neutron Scattering Studies. In *Methods in enzymology*, Vol. 565; Elsevier, 2015; pp 123-146.

(35) O'Neill, H.; Pingali, S. V.; Petridis, L.; He, J.; Mamontov, E.; Hong, L.; Urban, V.; Evans, B.; Langan, P.; Smith, J. C.; et al. Dynamics of water bound to crystalline cellulose. *Scientific Reports* **2017**, *7* (1), 11840. DOI: 10.1038/s41598-017-12035-w.

(36) Grusak, M. A. Intrinsic stable isotope labeling of plants for nutritional investigations in humans. *Journal of Nutritional Biochemistry* **1997**, *8* (4), 164-171. DOI: Doi 10.1016/S0955-2863(97)00017-X.

(37) Bhagia, S.; Nunez, A.; Wyman, C. E.; Kumar, R. Robustness of two-step acid hydrolysis procedure for composition analysis of poplar. *Bioresource Technology* **2016**, *216*, 1077-1082. DOI: 10.1016/j.biortech.2016.04.138.

(38) Kumar, R.; Hu, F.; Hubbell, C. A.; Ragauskas, A. J.; Wyman, C. E. Comparison of laboratory delignification methods, their selectivity, and impacts on physiochemical characteristics of cellulosic biomass. *Bioresource Technology* **2013**, *130*, 372-381. DOI: 10.1016/j.biortech.2012.12.028.

(39) Bhagia, S.; Pu, Y.; Evans, B. R.; Davison, B. H.; Ragauskas, A. J. Hemicellulose characterization of deuterated switchgrass. *Bioresource Technology* **2018**, *269*, 567-570. DOI: 10.1016/j.biortech.2018.08.034.

(40) Mazumder, K.; Peña, M. J.; O'Neill, M. A.; York, W. S. Structural characterization of the heteroxylans from poplar and switchgrass. In *Biomass Conversion*, Springer, 2012; pp 215-228.

(41) Bhagia, S.; Nunez, A.; Wyman, C. E.; Kumar, R. Robustness of two-step acid hydrolysis procedure for composition analysis of poplar. *Bioresource Technology* **2016**, *216*, 1077-1082. DOI: 10.1016/j.biortech.2016.04.138.

(42) Heller, W. T.; Urban, V. S.; Lynn, G. W.; Weiss, K. L.; O'Neill, H. M.; Pingali, S. V.; Qian, S.; Littrell, K. C.; Melnichenko, Y. B.; Buchanan, M. V.; et al. The Bio-SANS instrument at the High Flux Isotope Reactor of Oak Ridge National Laboratory. *Journal of Applied Crystallography* **2014**, *47* (4), 1238-1246. DOI: 10.1107/S1600576714011285.

(43) Heller, W. T.; Cuneo, M.; Debeer-Schmitt, L.; Do, C.; He, L. L.; Heroux, L.; Littrell, K.; Pingali, S. V.; Qian, S.; Stanley, C.; et al. The suite of small-angle neutron scattering instruments at Oak Ridge National Laboratory. *Journal of Applied Crystallography* **2018**, *51* (2), 242-248. DOI: 10.1107/S1600576718001231.

(44) Ilavsky, J.; Jemian, P. R. Irena: tool suite for modeling and analysis of small-angle scattering. *Journal of Applied Crystallography* **2009**, *42* (2), 347-353. DOI: 10.1107/S0021889809002222.

(45) Beaucage, G. Small-angle scattering from polymeric mass fractals of arbitrary mass-fractal dimension. *Journal of Applied Crystallography* **1996**, *29* (2), 134-146. DOI: 10.1107/S0021889895011605.

(46) Beaucage, G. Approximations leading to a unified exponential power-law approach to small-angle scattering. *Journal of Applied Crystallography* **1995**, *28* (6), 717-728. DOI: 10.1107/S0021889895005292.

(47) Fernandes, A. N.; Thomas, L. H.; Altaner, C. M.; Callow, P.; Forsyth, V. T.; Apperley, D. C.; Kennedy, C. J.; Jarvis, M. C. Nanostructure of cellulose microfibrils in spruce wood. *Proceedings of the National Academy of Sciences of the United States of America* **2011**, *108* (47), E1195-1203. DOI: 10.1073/pnas.1108942108.

(48) Langan, P.; Petridis, L.; O'Neill, H. M.; Pingali, S. V.; Foston, M.; Nishiyama, Y.; Schulz, R.; Lindner, B.; Hanson, B. L.; Harton, S.; et al. Common processes drive the thermochemical pretreatment of lignocellulosic biomass. *Green Chemistry* **2014**, *16* (1), 63-68. DOI: 10.1039/c3gc41962b.

(49) Pingali, S. V.; Urban, V. S.; Heller, W. T.; McGaughey, J.; O'Neill, H. M.; Foston, M.; Myles, D. A.; Ragauskas, A. J.; Evans, B. R. SANS study of cellulose extracted from switchgrass. *Acta Crystallography* **2010**, *66* (Pt 11), 1189-1193. DOI: 10.1107/S0907444910020408.

(50) Semeraro, E. F.; Marx, L.; Mandl, J.; Frewein, M. P. K.; Scott, H. L.; Prevost, S.; Bergler, H.; Lohner, K.; Pabst, G. Evolution of the analytical scattering model of live Escherichia coli. *Journal of Applied Crystallography* **2021**, *54* (2), 473-485. DOI: 10.1107/S1600576721000169.

(51) Semeraro, E. F.; Marx, L.; Mandl, J.; Letofsky-Papst, I.; Mayrhofer, C.; Frewein, M. P. K.; Scott, H. L.; Prévost, S.; Bergler, H.; Lohner, K.; et al. Lactoferricins impair the cytosolic membrane of Escherichia coli within a few seconds and accumulate inside the cell. *eLife* **2022**, *11*, e72850. DOI: 10.7554/eLife.72850.

(52) Hicks, A.; Abraham, P.; Leite, W.; Zhang, Q.; Weiss, K. L.; O'Neill, H.; Petridis, L.; Smith, J. C. SCOMAP-XD: atomistic deuterium contrast matching for small-angle neutron scattering in biology. *Acta Crystallographica Section D* **2023**, *79* (5), 420-434. DOI: 10.1107/S2059798323002899.

(53) Simon, C.; Morel, O.; Neutelings, G.; Baldacci-Cresp, F.; Baucher, M.; Spriet, C.; Biot, C.; Hawkins, S.; Lion, C. Exploring Lignification Complexity in Plant Cell Walls with Airyscan Super-resolution Microscopy and Bioorthogonal Chemistry. *Chemical & Biomedical Imaging* **2023**, *1* (5), 479-487. DOI: 10.1021/cbmi.3c00052.

(54) Wypych, A. *Databook of Adhesion Promoters*; ChemTec Publishing, 2018. DOI: 10.1016/B978-1-927885-27-7.50018-1.

(55) Hodge, A.; Berta, G.; Doussan, C.; Merchan, F.; Crespi, M. Plant root growth, architecture and function. *Plant and Soil* **2009**, *321* (1-2), 153-187. DOI: 10.1007/s11104-009-9929-9.

(56) Voragen, F.; Schols, H.; Visser, R. *Advances in Pectin and Pectinase Research*; Springer, 2003. DOI: 10.1007/978-94-017-0331-4.

(57) Shrestha, U. R.; Smith, S.; Pingali, S. V.; Yang, H.; Zahran, M.; Breunig, L.; Wilson, L. A.; Kowali, M.; Kubicki, J. D.; Cosgrove, D. J.; et al. Arabinose substitution effect on xylan rigidity and self-aggregation. *Cellulose* **2019**, *26* (4), 2267-2278. DOI: 10.1007/s10570-018-2202-8.

(58) Kumar, R.; Bhagia, S.; Smith, M. D.; Petridis, L.; Ong, R. G.; Cai, C. M.; Mittal, A.; Himmel, M. H.; Balan, V.; Dale, B. E.; et al. Cellulose-hemicellulose interactions at elevated temperatures increase cellulose recalcitrance to biological conversion. *Green Chemistry* **2018**, *20* (4), 921-934. DOI: 10.1039/c7gc03518g.

(59) Mansfield, S. D.; Kim, H.; Lu, F.; Ralph, J. Whole plant cell wall characterization using solution-state 2D NMR. *Nature Protocols* **2012**, *7* (9), 1579-1589. DOI: 10.1038/nprot.2012.064.

(60) Lu, F.; Ralph, J. Non-degradative dissolution and acetylation of ball-milled plant cell walls: high-resolution solution-state NMR. *Plant Journal* **2003**, *35* (4), 535-544. DOI: 10.1046/j.1365-313x.2003.01817.x.

Tables:

Table 1. Compositional analysis of extractives free protiated kale stem[⊥]

Cellulose	Xylan	Ash	Others[+]
28.2 ± 0.2	11.8 ± 0.2	5.6	55.0

[⊥] Unit for all values are percent weight, wt%; Lignin content were below the accuracy limit of the analytical balance.
[+] Includes polysaccharides like hemicellulose other than xylan (arabinose, glucuronic acid), pectin (homogalacturonan, rhamnogalacturonan), and acetyl groups.

Table 2. Fourier-transform Infrared – Attenuated Total Reflection (FTIR-ATR) Spectroscopy data of deuterated kale stem and its component plant biopolymers.

Sample/Ratios	C-D/C-H	O-D/O-H
d-kale stem (Extractives Free)	0.384	0.145
Cellulose	0.464	0.244
Hemicellulose (Xylan)	0.273	-
Lignin*	0.258	0.137

* Trace quantities of lignin recovered after removal of the polysaccharides was sufficient for FTIR-ATR measurements but *not* sufficient for estimation of lignin content.

Table 3. Unified fit structural parameters of the SANS data of deuterated kale stem and cellulose extracted deuterated kale in 0% D_2O solvent.

Sample	Structural Level	Length Scale Range*^ (Å)	Q-range (Å^{-1})	Radius of Gyration, R_g (Å)	Power-law exponent, P
d-kale stem	1	2.5 - 20	0.05 - 0.4	15 ± 1	4[#]
	2	20 - 166	0.006 - 0.05		2.10 ± 0.04
	3	166 - 333	0.003 - 0.006		4[#]
Cellulose extracts	1	2.5 - 25	0.04 - 0.4	24 ± 3	4[#]
	2	25 - 200	0.005 - 0.04	190 ± 28	2.5 ± 0.2
	3	200 - 333	0.003 - 0.005		2.4 ± 0.2

*The values for 'Length Scale Range' were calculated using the relation $1/Q$ (Å^{-1}) to determine the range of accessible particle sizes in each Q-range.
^The 'length scale range' for correlation distance (or particle-particle distance), d, accessible for the same set of Q-ranges is obtained using the relation d (Å) = $2\pi/Q$ (Å^{-1}). This length scale range is used to interpret sizes of features responsible for the power-law behavior (surface and bulk morphology).
#Parameters with a fixed value during fit.

Figure captions

Figure 1.

FTIR spectra of deuterated kale stem and its cellulose, hemicellulose, and lignin extracts. The spectra are vertically shifted for clarity.

Figure 2.

SANS profiles for contrast variation study of deuterated kale stems (A) and extracted cellulose (B). Inset in (A) and (B) shows a plot of square-root of scattering intensity for a fixed Q (= 0.05 $Å^{-1}$) versus D_2O content of the solvent. A linear fit to the data shows zero contrast is obtained for 63.7% D_2O (A) and 69.4 % D_2O (B) for Q=0.05 $Å^{-1}$. (C, D) SANS profile of deuterated kale stem (C) and its extracted cellulose (D) in 0% D_2O. The lines in (C, D) represent the composite Unified Fit (solid black line) and its three individual levels (Level 1: dashed green, Level 2: dashed blue, Level 3: dashed magenta).

Figure 3.

Contrast matching D_2O% as a function of scattering vector Q for deuterated kale stem (red dot) and its cellulose extracts (blue triangle).

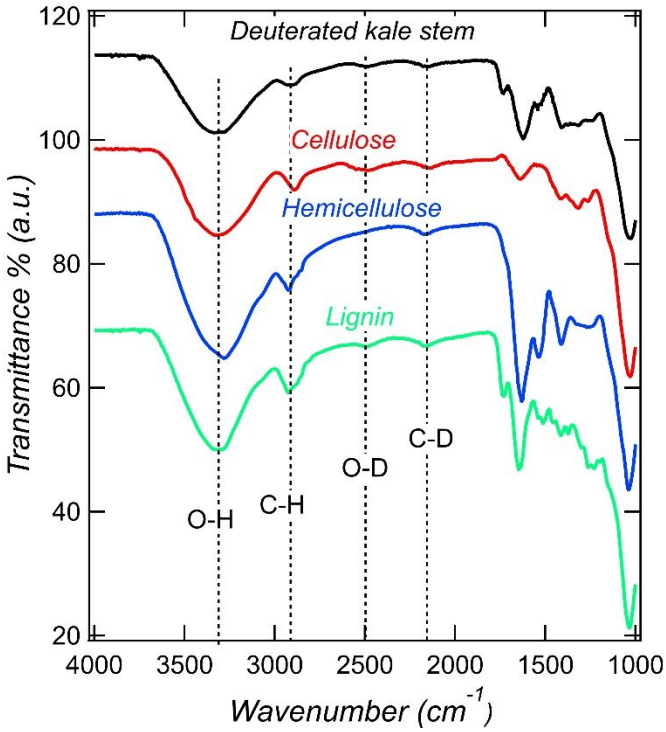
Deuterated kale stem
Cellulose
Hemicellulose
Lignin
O-H
C-H
O-D
C-D
Transmittance % (a.u.)
Wavenumber (cm-1)
120
100
80
60
40
20
4000
3500
3000
2500
2000
1500
1000

Figure 1.

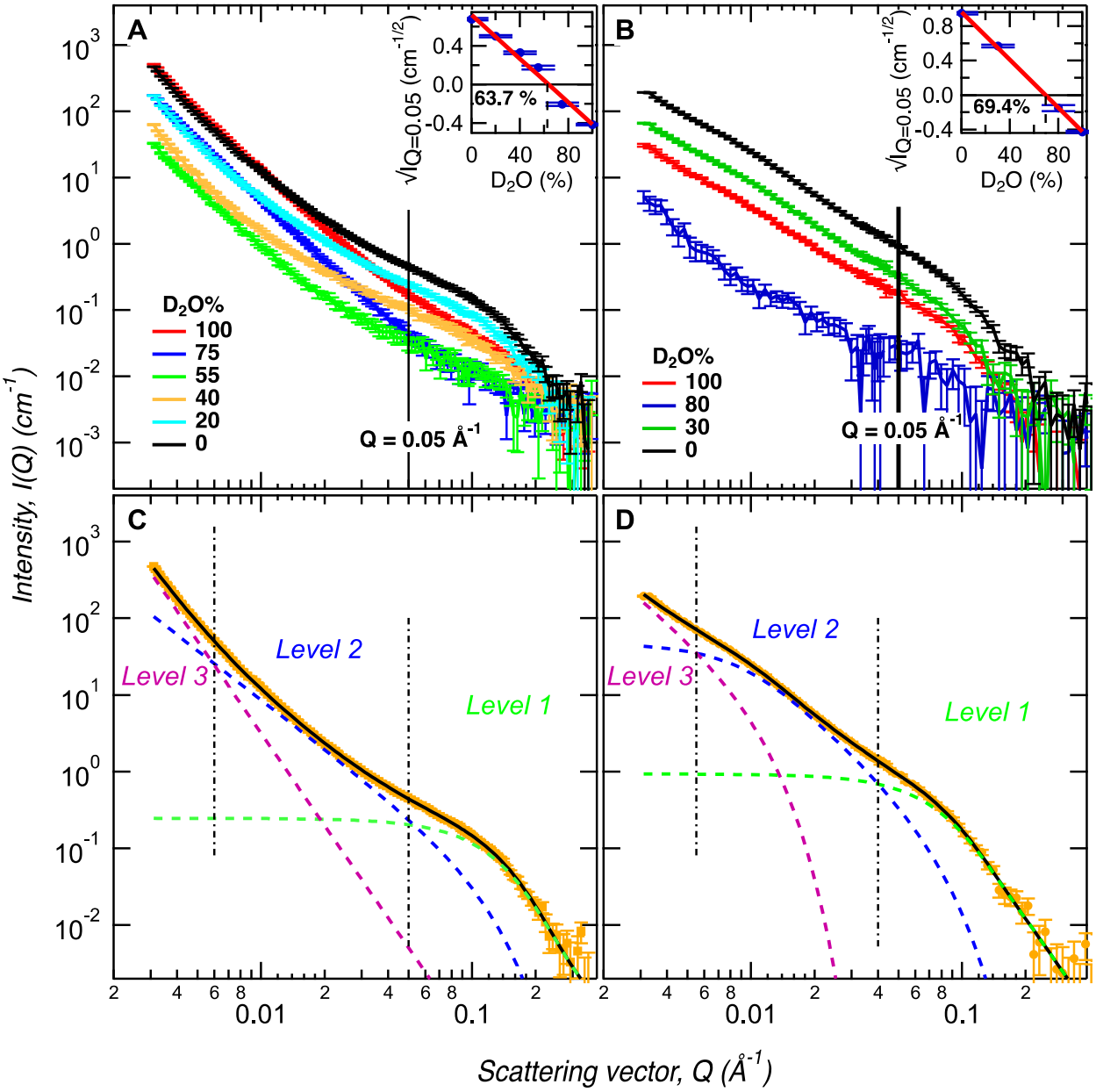
A
B
C
D
Intensity, I(Q) (cm-1)
Scattering vector, Q (Å-1)
D2O%
100
75
55
40
20
0
80
30
Q = 0.05 Å-1
√IQ=0.05 (cm-1/2)
D2O (%)
63.7 %
69.4%
Level 1
Level 2
Level 3
0.01
0.1

Figure 2.

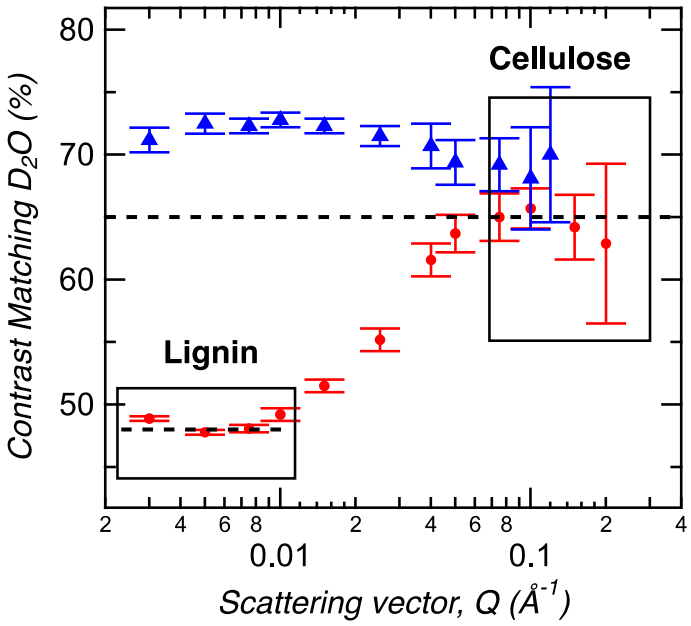
Cellulose
Lignin
Contrast Matching D_2O (%)
Scattering vector, Q (Å^{-1})
80
70
60
50
0.01
0.1

Figure 3.

For Table of Contents Use Only

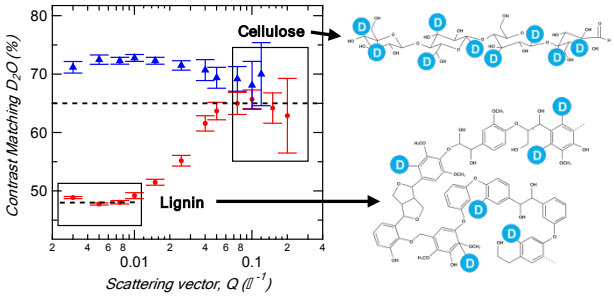

Synopsis:

Growing partially deuterated kale plant shows differential incorporation of deuterium into component biopolymers enabling deconvolution of the complex cell wall structure.